Journal of Microscopy, Vol. 189, Pt 1, January 1998, pp. 8–11.
Received 14 August 1997; accepted 30 September 1997

SHORT COMMUNICATION

The measurement of the amplitude point spread function of microscope objective lenses

R. JUŠKAITIS & T. WILSON
Department of Engineering Science, University of Oxford, Parks Road, Oxford OX1 3PJ, U.K.

Key words. Amplitude, confocal microscopy, fibre optic interferometer, point spread function.

Summary

We present a simple method of directly measuring the complex amplitude point spread function of a microscope objective lens. The method is based on an optical fibre interferometer. Experimental results are presented for a high-aperture water-immersion objective lens.

1. Introduction

The limiting factor which ultimately determines the ability of a microscope to produce a good image is the quality of the objective lens. Any imperfections or aberrations present will lead to a degraded image. This is particularly important in confocal microscopy and multiphoton microscopies since objective lens phase aberrations have a much greater effect on image quality and signal level in these instruments than they do in conventional wide-field systems. It is therefore important to be able to measure the amplitude and phase of the amplitude point spread function of an objective lens in a simple manner. There are, of course, many interferometric

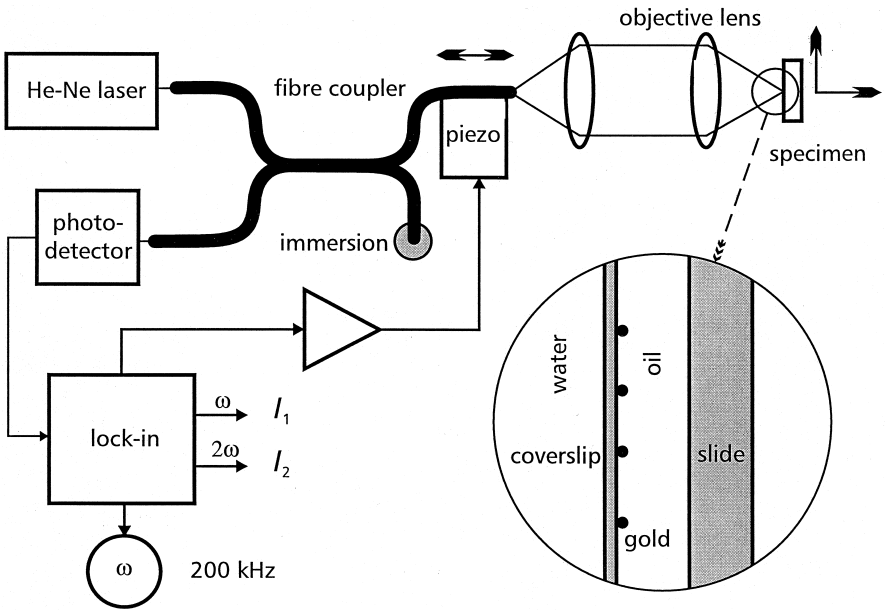

Fig. 1. Schematic diagram of the confocal interference microscope.

Fig. 2. The amplitude and phase of the effective point spread function for the case of three settings of the cover glass correction collar, D (μm). The image size is $5\,\mu m \times 5\,\mu m$. The horizontal axis corresponds to the lateral coordinate (x) and the vertical axis corresponds to the axial coordinate (z).

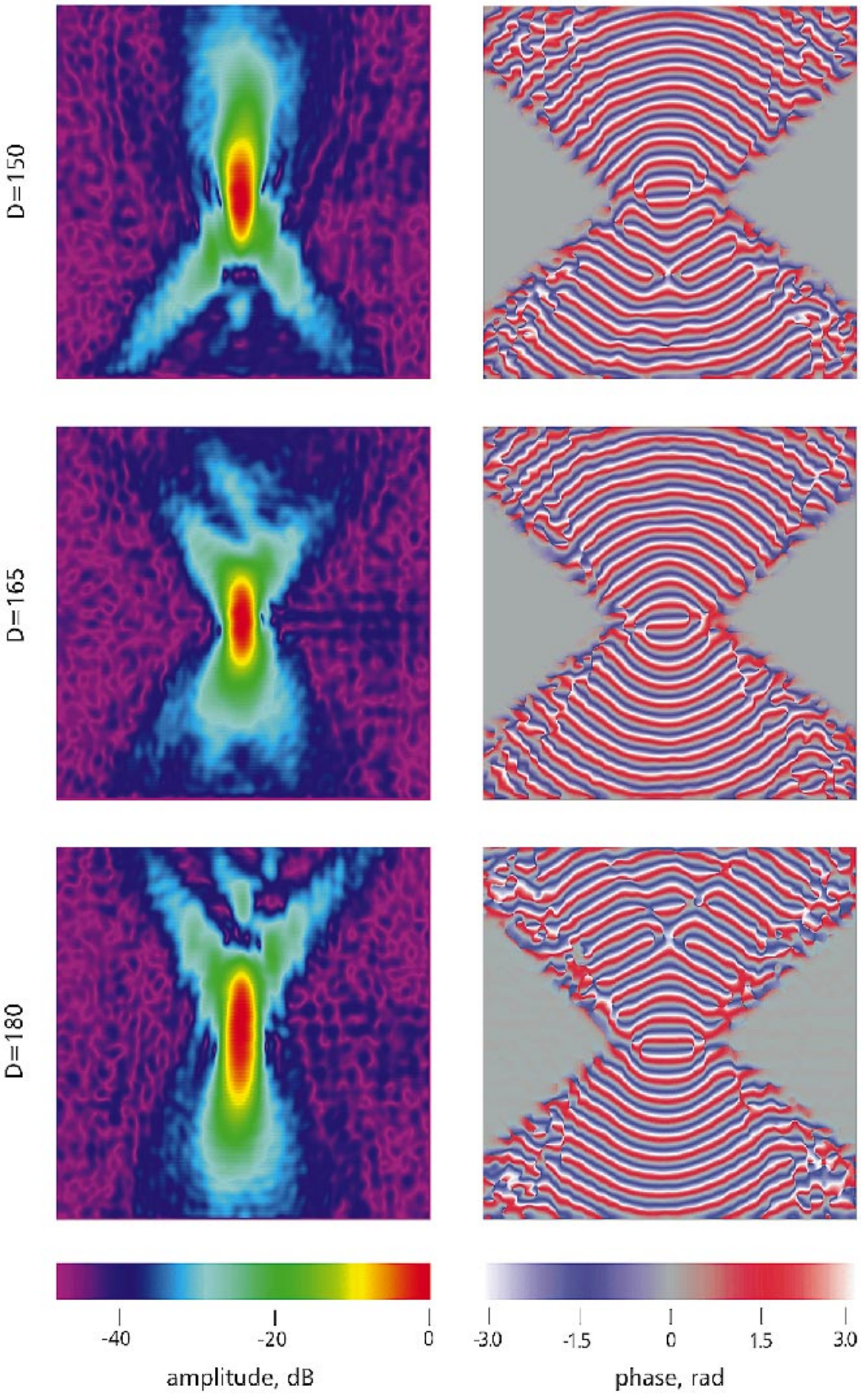

methods which either compare the wavefronts produced by the lens with a reference or which simply record an interference image of a point object (Twyman & Green, 1916; Schrader & Hell, 1996). However, none of these methods extracts directly the full complex amplitude point spread function. In the following we will present a new method based on a fibre optic interferometer which permits us to recover the full complex point spread function.

2. Preliminary considerations

Our approach is to build an interference microscope and to extract both the amplitude and the phase of the amplitude point spread function from the interference image of a subresolution point scatterer. In principle, any configuration of interference microscope may be used but those based on the Michelson geometry in reflection (Wilson & Sheppard, 1984; Wilson & Juškaitis, 1994) or the Mach–Zender configuration in transmission (Brakenhoff, 1979) are not common path systems and hence are extremely sensitive to spurious air currents etc. The system shown in Fig. 1 is an almost common path interference microscope based on the use of a single mode optical fibre (Wilson *et al.*, 1994) which does not suffer from these drawbacks. The fibre serves both to launch the light into the microscope and to detect the reflected confocal field amplitude. We do not index-match the fibre tip to the microscope optics and so part of the incident light is reflected back along the fibre at the tip; this forms the reference beam. Since both the object and reference beams propagate back in the same fibre mode their phase fronts are perfectly matched when they interfere on the photodetector. The detected signal is now given by

$$I = |r + U|^2 \tag{1}$$

where r denotes the amplitude of the reference beam and U is the confocal amplitude signal.

In order to be able to extract the complex field, U, from the interference signal, I, we introduce a very small amplitude dither to the fibre tip so as to introduce a time-varying phase shift $\phi(t) = \phi_0 \cos(\omega t)$ into the object beam. Equation (1) now takes the form

$$\begin{aligned} I &= |r + U \exp j\phi(t)|^2 \\ &= r^2 + |U|^2 + 2r\{Re\{U\} \cos(\phi_0 \cos \omega t) \\ &\quad - Im\{U\} \sin(\phi_0 \cos \omega t)\} \end{aligned} \tag{2}$$

where we have assumed r to be real for simplicity. It is now a simple matter to extract both $Re\{U\}$ and $Im\{U\}$ from this signal by standard synchronous demodulation (or lock-in detection) techniques. If we multiply Eq. (2) by $\cos(\omega t)$ and time-average the result we obtain (Wilson *et al.*, 1994)

$$I_1 \sim Im\{U\} \tag{3}$$

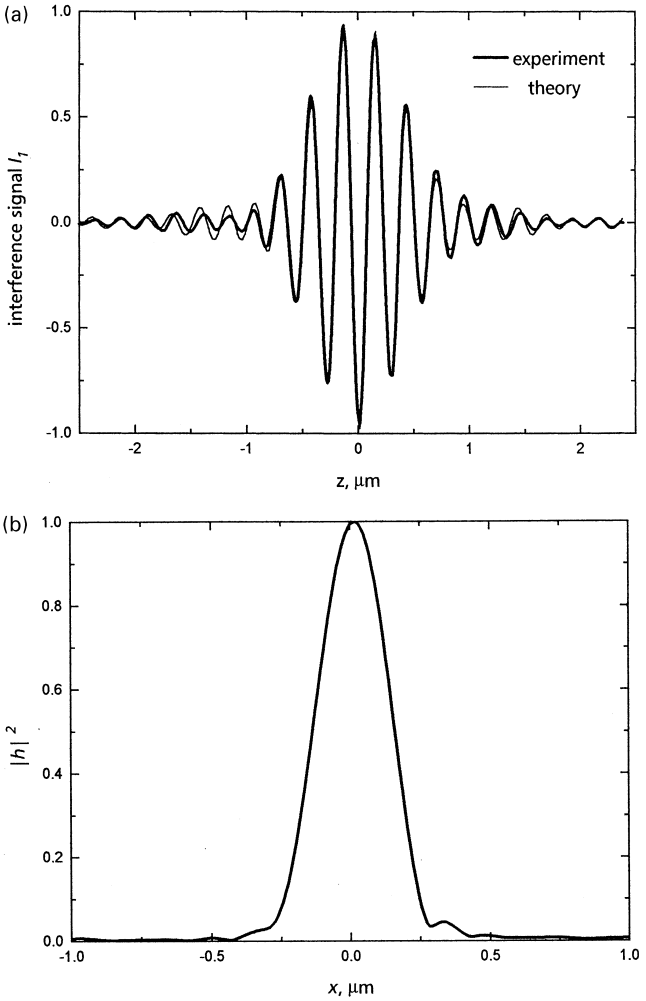

Fig. 3. (a) The variation of the raw interferometric signal, I_1, along the optical axis. (b) The variation of h^2 in the focal plane.

whereas synchronous demodulation with $\cos(2\omega t)$ yields

$$I_2 \sim Re\{U\}. \tag{4}$$

Further, if the object is a point scatterer then

$$U = h_{\text{eff}} = h^2 \tag{5}$$

where h_{eff} is the effective amplitude point spread function of the confocal microscope and h is the amplitude point spread function of the objective lens. We see that we are now able to obtain two quadrature interference images I_1 and I_2 that contain all the information which permits us to recover the amplitude and phase of the amplitude point spread function of the objective lens.

3. Experimental

In order to demonstrate the effectiveness of our method we elected to measure the amplitude point spread function

of an Olympus 60×, 1·2-NA WPSF water-immersion objective lens. This objective lens also has a collar to correct for cover glass thicknesses in the range 0·14–0·21 mm. Our point scatterer was a 100-nm colloidal gold bead which was mounted beneath a #1·5 cover slip of nominal thickness 0·17 mm. The cover slip with beads was in turn mounted on a microscope slide and the gap between them was filled with immersion oil so as to eliminate reflection from the back surface of the cover glass, Fig. 1. The size of bead was carefully chosen experimentally so as to maximize the signal level but without compromising the point-like behaviour. For comparison the experiment was repeated using a 40-nm bead and similar results to those presented here were obtained but with a vastly inferior signal-to-noise ratio. Full calculations based on Mie scattering theory also confirmed that the 100-nm bead in this configuration behaves as a point scatterer. The fibre tip was mounted on a piezoelectric modulator and dithered at 200 kHz. For convenience the whole system was built around a single mode fibre optic beam splitter, the second output of which was index-matched to remove the unwanted reflection. A helium–neon laser (633 nm wavelength) was used as a light source.

The amplitude and phase of the effective point spread function was extracted from the two quadrature x–z scan images, I_1 and I_2, and the results are presented in Fig. 2 for three settings of the cover slip correction collar. In order to emphasize the side lobe structure the amplitude of the point spread function is displayed in dBs as $20\log_{10}\{h_{\text{eff}}\}$. We see that a correction collar setting of 0·165 mm gives an optimum form to the point spread function. An incorrect setting of the correction collar inevitably introduces aberrations into the system. This can be seen clearly in the top and bottom images in Fig. 2, which correspond to a 10% cover glass thickness mismatch above and below the optimum. Note the symmetric behaviour of the point spread functions to positive and negative aberration.

In Fig. 3 we show variation of one of the raw interferometric signals along the optical axis and h^2 in the focal plane. In the case of the axial distribution we also show a theoretical fit to the experimental result. The theory used was similar to that presented in Wilson *et al.* (1994) and the fit shown here was obtained by assuming a numerical aperture of 1·15 rather than the nominal value of 1·2. The full width at half-maximum was measured to be 0·3 μm, which compares well with the theoretical value of 0·28 μm for a 1·15-NA objective lens.

4. Conclusions

We have presented a simple method which permits the direct measurement of the amplitude point spread function of a high-aperture microscope objective with great precision. We note a dynamic range of greater than 40 dB in the results shown in Fig. 2. The particular high-aperture water-immersion lens which we tested was found to perform well when the cover glass correction collar was correctly set but aberration was inevitably introduced for incorrect settings.

Acknowledgment

We thank Dr M. A. A. Neil for his help in the preparation of Fig. 3(a).

References

Brakenhoff, G.J. (1979) Imaging modes in confocal scanning light microscopy. *J. Microsc.* **117,** 233.

Schrader, M. & Hell, S.W. (1996) Wavefronts in the focus of a light microscope. *J. Microsc.* **184,** 143–148.

Twyman, F. & Green, A. (1916) British Patent No. 103832.

Wilson, T. & Juškaitis, R. (1994) Scanning interference microscopy. *Bioimaging,* **2,** 36–40.

Wilson, T., Juškaitis, R., Rea, N.P. & Hamilton, D.K. (1994) Fibre optic interference and confocal microscopy. *Opt. Commun.* **110,** 1–6.

Wilson, T. & Sheppard, C.J.R. (1984) *Theory and Practice of Scanning Optical Microscope*. Academic Press, London.